UCRL-TR-210700

LAWRENCE
LIVERMORE
NATIONAL
LABORATORY

Advanced Crystal Growth Technology

T. A. Land, R. A. Hawley-Fedder

March 21, 2005

Disclaimer

FY04 LDRD Final Report
Advanced Crystal Growth Technology
LDRD Project Tracking Code: 02-ERD-70
Teresa A. Land, C0-Principal Investigator
Ruth Hawley-Fedder, Principal Investigator

Abstract

Although the fundamental mechanism of crystal growth has received and continues to receive deserved attention as a research activity, similar research efforts addressing the need for advanced materials and processing technology required to grow future high quality crystals has been sorely lacking. The purpose of this research effort is to develop advanced rapid growth processing technologies and materials suitable for providing the quality of products needed for advanced laser and photonics applications. In particular we are interested in developing a methodology for growing high quality KDP crystals based on an understanding of the fundamental mechanisms affecting growth.

One problem in particular is the issue of control of impurities during the growth process. Many unwanted impurities are derived from the growth system containers and can adversely affect the optical quality and aspect ratio (shape) of the crystals. Previous studies have shown that even trace concentrations ($\sim 10^{-9}$ M) of impurities affect growth and even "insignificant" species can have a large impact. It is also known that impurities affect the two growth faces of KDP very differently. Traces of trivalent metal impurities such as Fe^{3+}, Cr^{3+}, and Al^{3+} in solution are known to inhibit growth of the prismatic {100} faces of KDP while having little effect on the growth of the pyramidal {101} faces. This differentiation opens the possibility of intentionally adding select ions to control the aspect ratio of the crystal to obtain a more advantageous shape.

This document summarizes our research efforts to improve KDP crystal growth. The first step was to control unwanted impurity addition from the growth vessel by developing an FEP liner to act as a barrier to the glass container. The other focus to develop an understanding of select impurities on growth rates in order to be able to use them to control the habit or shape of the crystal for yield improvement.

Research Activities

FEP lined tanks were developed to control impurity levels in the growth solution

Prior to mid-2003, rapid growth of KDP crystals was performed in glass tanks. The presence of the glass solution interface is known to allow glass components to enter the growth solution. It is well established that trace elements from the glass can influence the course of a growth run. This has confounded the understanding of historical large KDP growth runs. This dissolution made control of the exact chemical composition of the growth solution problematic. Since crystal growth habit is a function of trivalent cation concentration and the glass contained significant quantities of trivalent aluminum, determining the influence of process

variables on growth geometry was difficult. Investigations begun in FY02 focused on control of impurities through the use of engineered barriers. We chose to investigate development of an engineered impurity barrier for the glass growth tank to retard or inhibit the release of impurities from the tank walls. In FY03 an FEP liner was developed and tested in large-scale experimentation. Over the last two years there has been over 25 large KDP crystal growth runs in Teflon (FEP) lined growth tanks. The lining removes the problem of glass dissolution into the growth solution. Thus this new data, we believe, represents a simplified data set and allows us the opportunity to take a fresh look at the large-crystal growth process [1,2].

The first crystals grown in lined tanks had very low aspect ratios that were very unfavorable for plate yield. It turns out that impurities from the glass were strongly incorporated into the prism faces and slowed this growth rate relative to the pyramid face creating high aspect ratio crystals but levels of impurities negatively affected the quality. The lined tanks allowed us explore the use selective 'impurity' addition to control the crystal aspect ratio. We determined that aluminum could be added to the growth solution at controlled levels without negatively affecting the material quality while improving the aspect ratio. In order to make this improved "lined-tank" process successful, we had to understand the effects of temperature, aluminum concentration, supersaturation, and EDTA concentration on growth kinetics.

EDTA

The introduction of the FEP liner got rid of the unwanted chemical impurities from the glass growth vessel but a complex relation between the starting KDP salt and aluminum added to control the aspect ratio still exists. The raw material typically used for the growth of single crystal KDP is generally prepared by precipitating KDP from an aqueous solution containing H_3PO_4, KOH and about 1 mole% of the dipotassium salt of ethylenediaminetetraacetic acid [3]. The EDTA is used during the preparation of the KDP feedstock as a means of sequestering trace quantities of metallic species, such as iron, which are invariably present in the raw materials and may be introduced by glass growth vessels. During the precipitation of the KDP feedstock, a small fraction of the EDTA either co-precipitates or adsorbs to the surface of the KDP crystals. Thus growth solutions using "low impurity" KDP prepared by this method generally contain a small fraction of EDTA.

The EDTA in the growth solution can have a profound effect on the relative face growth rates and hence crystal shape as well as on the material quality and is important to understand. For example, if sufficient EDTA were present it could potentially complex with metallic cations, such as Al^{3+}, that are used to control the aspect ratio of KDP crystallization. It is reasonable to expect that, if this were the case, then not all aluminum species would be expected to be incorporated into the crystal lattice. Altering the speciation of metallic complexes by the introduction of EDTA could perturb the relative growth rates of the various crystal faces.

Initial results obtained in FY02 in using controlled addition of Al^{3+} to affect aspect ratio in KDP showed surprising results, indicating that other factors might compete with impurity effects to influence aspect ratio. Of particular significance in FY03 was the development of an improved understanding of the speciation chemistry of

trivalent cations (Al^{3+}) in the presence of KDP and EDTA. In particular a better understanding of the temperature and pH dependence of the formation of various Al-KDP complexes and Al-EDTA complexes has been critical to our investigations into the effect of Al^{3+} on aspect ratio [4]. Modeling of the complex equilibria present suggests that Al^{3+} preferentially binds to EDTA at high temperatures (>55°C), while at lower temperatures Al is less strongly bound by EDTA and incorporated into the growing crystal. Al^{3+} is present in solution primarily as $AlPO_4$ (85%) even in the presence of excess EDTA. This means that for Al^{3+} to be effective controlling aspect ratio, it must be introduced late in the growth run when temperatures are below 55°C. These results were confirmed by chemical analysis of KDP and DKDP crystals grown in the presence of Al at varying temperatures.

In the absence of EDTA, the dominant aluminum species in KDP growth solution would be expected to be $AlPO_4$. Minor quantities of $AlHPO_4^+$, and $AlH_2PO_4^{2+}$ would also be expected to be present. Introduction of small concentrations of EDTA (0.001-.03 mole% relative to KDP), at pHs of relevance to KDP growth, would be expected to result in a strong competition between the EDTA and the phosphate ion for the aluminum cations. Increasing the concentration of (unbound) EDTA would be expected to increase the fraction of the Al-EDTA complex, relative to the $AlPO_4$ complex.

Existing heats of reaction indicate that the formation of the Al-EDTA complex is strongly favored by increased temperatures. Although the temperature dependence of the reactions leading to the formation of the three aluminum phosphates are not known with certainty, there is good reason to suggest that the formation of $AlPO_4$ species is favored at lower temperatures (e.g. room temperature). If this is the case, reasonable arguments can be put forward to suggest that the speciation of aluminum might well be strongly disrupted, at elevated temperatures, by the presence of modest (0.001-0.03 mole%) concentrations of EDTA. Specifically, the presence of EDTA would be expected to have virtually no effect on growth solutions near room temperature, while at elevated temperatures a substantial fraction of the aluminum in solution would be expected to be present as the Al-EDTA, rather than as the $AlPO_4$ complex.

One would expect that the speciation of a given metallic ion or complex in solution would profoundly effect the ability of such a species to interact with a crystal, and thus influence its growth rate. Thus the competition between the phosphate and the EDTA, for aluminum cations, has a number of practical implications with respect to KDP growth. First, phenomenological parameters, such as the segregation coefficient (i.e. the concentration of Al in the crystal relative to the concentration of Al in solution) would be expected to show temperature dependence. If, for example, $AlPO_4$ were the species which most strongly interacts with the crystal lattice one would expect the segregation coefficient to decrease in proportion to the fraction of $AlPO_4$ in solution for a given total aluminum concentration. In the absence of EDTA, such a reduction would be expected to be relatively modest. Using the temperature dependence described above, one finds that the fraction of $AlPO_4$ in solution drops from about .96 at 25 °C to about .82 at 65 °C. In the presence of residual EDTA, however, a much more substantial temperature dependence might be expected. For example, with a salt containing 0.01mole% EDTA the fraction of aluminum present as $AlPO_4$ is about 95% at 25 °C, it is only about 5% abundant at 65 °C. Thus, other things being equal, the total concentration of Al that would be required to affect a specific crystal aspect ratio for

a crystal grown at 25 °C would be quite different than the total concentration needed to achieve the same degree of prismatic pinning, and thus aspect ratio at 75 °C. Equations defining the temperature dependence of Al incorporation into DKDP and KDP in the presence of EDTA were developed [4].

Flow cell investigation of impurity effect on face growth velocity

Face growth rate data from large tank crystal growth runs is complicated as there is both a mass transfer and kinetic component. In order to de-convolute the effect of various parameters on growth rate, a flow cell apparatus has been constructed to measure the rate of KDP crystal growth under conditions that are not limited by mass transfer and under conditions of constant temperature and supersaturation.

Kinetic measurements have been made using a flow cell apparatus, which was operated such that crystal growth took place without mass transfer limitations [5]. Crystals were grown from solutions that were free from impurities, solutions spiked with aluminum and EDTA. Measurements of the kinetics of KDP growth, from 30 to 58ºC with varying aluminum and EDTA concentrations are shown in ref [5].

From the data shown in ref [5], it is evident that doping KDP growth solutions with aluminum retards the rate of prism growth, while at the same time causes little, if any, change in the pyramidal growth rate. To illustrate the dependence of prism growth rate on aluminum concentration in the growth solution, the average prism face velocity is plotted as a function of aluminum concentration normalized by the face velocity at zero aluminum concentration in Figure 1. Normalizing the data in this way allows the three sets of conditions to be directly compared.
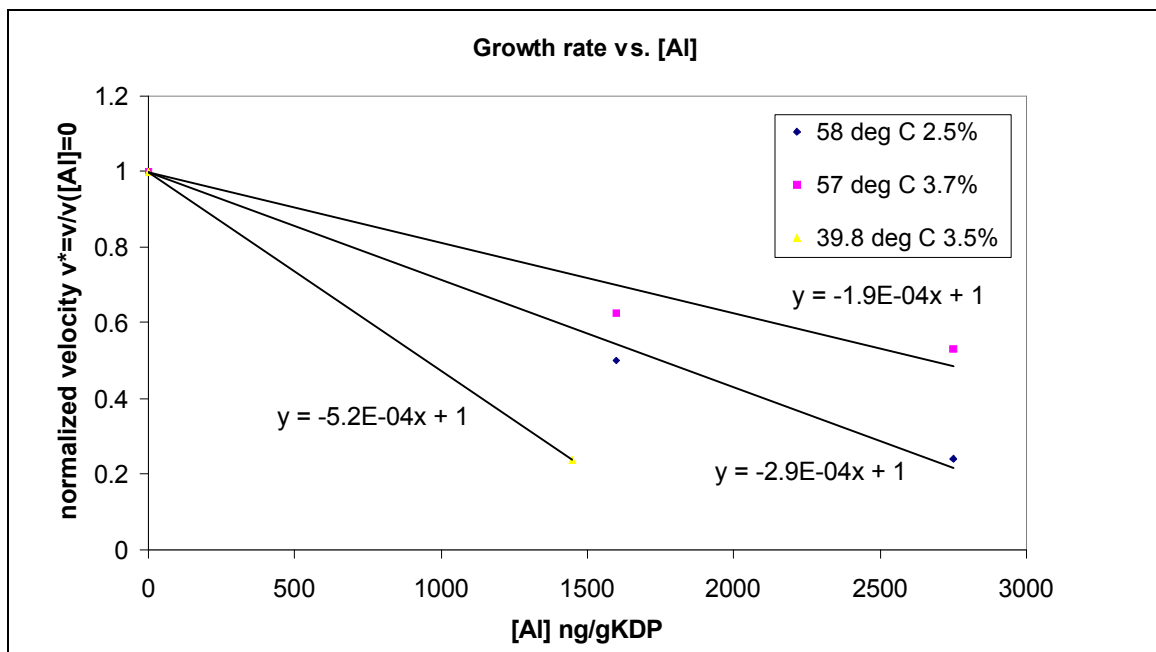

Growth rate vs. [Al]

Legend:
- 58 deg C 2.5%
- 57 deg C 3.7%
- 39.8 deg C 3.5%

$y = -1.9E\text{-}04x + 1$

$y = -5.2E\text{-}04x + 1$

$y = -2.9E\text{-}04x + 1$

x-axis: [Al] ng/gKDP
y-axis: normalized velocity v*=v/v([Al]=0)

Figure 1: Chart showing the effect of aluminum concentration in the growth

solution on the growth rate of the crystal prisms where the face velocities at three sets of temperature and concentration conditions have been normalized by their velocities with no aluminum in solution.

In addition to examining the effect that doping aluminum into growth solutions has on growth rates, the effect that the addition of EDTA has on growth rates in aluminum doped solutions has been explored. The data shows that spiking an aluminum doped growth solutions with EDTA does appear to increase the average prismatic growth rate, relative to an Al doped, EDTA free solution. In previous work, it was predicted that at elevated temperatures EDTA would compete more effectively against phosphate ions for Al^{3+} cations in solution. Therefore, it was predicted that addition of EDTA to growth solutions, spiked with aluminum, would reduce the effective Al concentration and thus reduce the number of prismatic growth sites pinned by Al cations.

At approximately 40ºC and 3.5% supersaturation, the effect of adding EDTA to a solution spiked with 1450 ng Al/ g KDP was to increase the rate of the prisms relative to the EDTA free solution by about 30%. Similarly, a 40% increase in prism growth was observed after EDTA was added in the experiment at 58ºC, 2.6% supersaturation, and 2750 ng Al/ g KDP. However, adding EDTA had no significant effect on the growth rate of crystal prisms grown at 57ºC, 3.8% supersaturation, and 2750 ng Al/ g KDP. These data suggest that the effect of the EDTA remains quite modest at these temperatures.

Atomic force microscopy investigation of impurity effects on step morphology and growth kinetics

Impurity adsorbates can induce drastic changes in the growth behavior of crystal surfaces, including reduction of growth rate, changes in the crystal habit, and changes in the step morphology [7-17]. Well-characterized systems, such as KDP, where some of the key variables can be isolated make excellent model systems to better understand the complexity of the interactions between adsorbates and surfaces.

Research on the effects of impurity adsorbates using interferometry and research in this study using AFM revealed the presence of a velocity dead zone caused by adsorption of aqueous complexes of Al(III), Fe(III) and Cr(III). Interferometric experiments revealed that Fe(III) caused a velocity dead zone that was not predicted by the C-V model, but the source of the deviation could not be explained. The use of AFM revealed morphological changes in addition to the velocity data that may explain the dependence of step velocity on supersaturation. Growth of the {100} face occurs via three distinct step classes: *elementary* steps, *macrosteps,* and *supersteps*, which are bunches of fifty to several hundreds of elementary steps [8,9,12-16].

Effect on Step Velocity and Morphology:
The step velocity-vs.-supersaturation curves for pure KDP growth, and solutions doped with Fe(III), Al(III), and Cr(III), are given in Figure 2 a-d, respectively. Due to the amount of data collected for the pure KDP system, these data are presented in Figure 2 a as a curve indicating mean velocities with error bars corresponding to

the 95% confidence interval. The locations of σ* and σ_d are shown in Figure 2a as a basis of comparison for following figures. The key points of the step velocity vs. supersaturation curve, shown in Figure 2b, illustrate the region of the growth curve where the images from Figure 3 are approximately located.
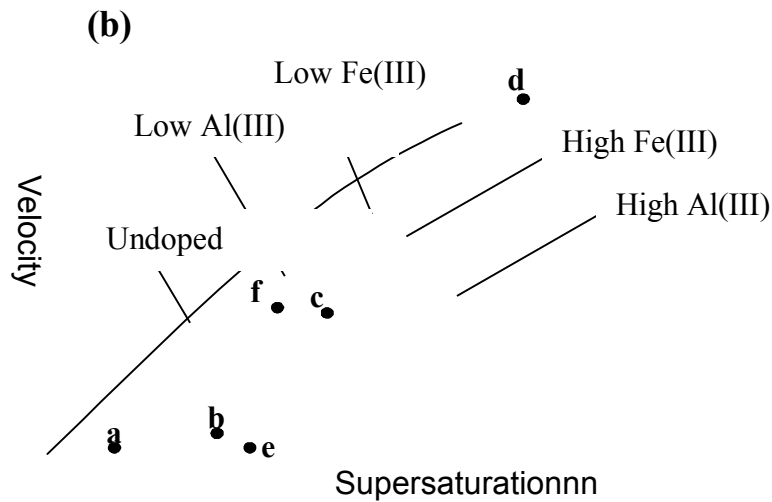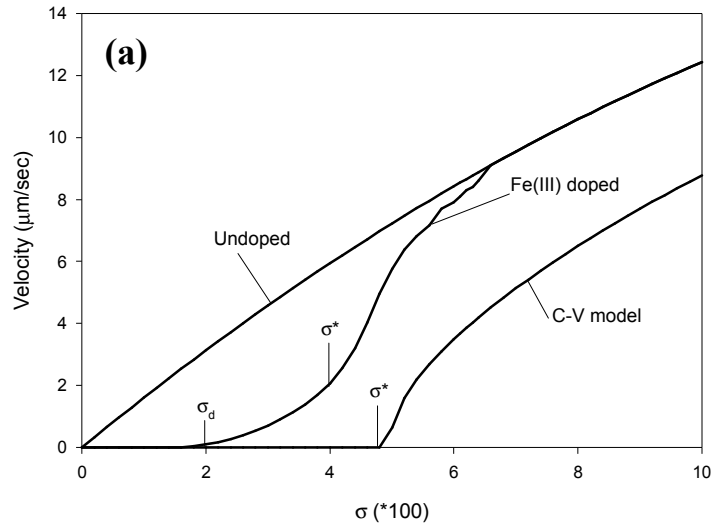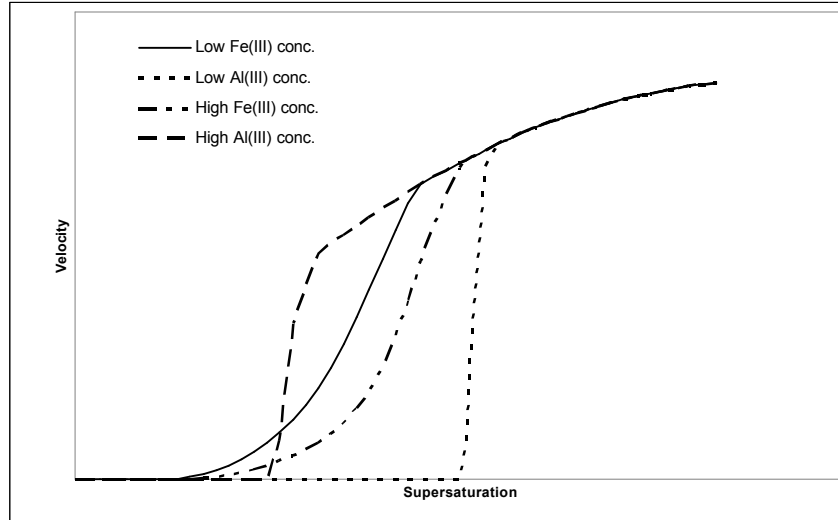
Figure 2 a) Comparison of the dependence of V on σ for growth from an undoped solution, doped with Fe(III), and in the presence of adsorbates as predicted by the C-V model. The Fe(III) and C-V curves are labeled with the locations of σ* and σd. (b) Schematic of dependence of V on σ for Al(III) and Fe(III) a dead zone (Region a). For Fe(III)-doped surfaces, the velocity curve has a roughly linear region of slow growth that is not predicted by the C-V model (region b), followed by a rapid rise in velocity (region c). after which the velocity rejoins that of the undoped system (region d). The shape of the velocity curves for surfaces grown in the presence of Al(III) have a shape that is at least qualitatively similar to that predicted by the C-V model, but in fact, as we will show later, do not quantitatively fit the C-V prediction.   The curves for both exhibit a dead zone at low supersaturations (region a), a critical supersaturation, $\sigma*$ where growth suddenly begins (point e), and a rapid rise in velocity (region f) after which the velocity curve rejoins that of the clean curve (region d). Cr(III) curves are the same shape as the Al(III) curves. The finely dotted line is a typical growth curve from an undoped solution.
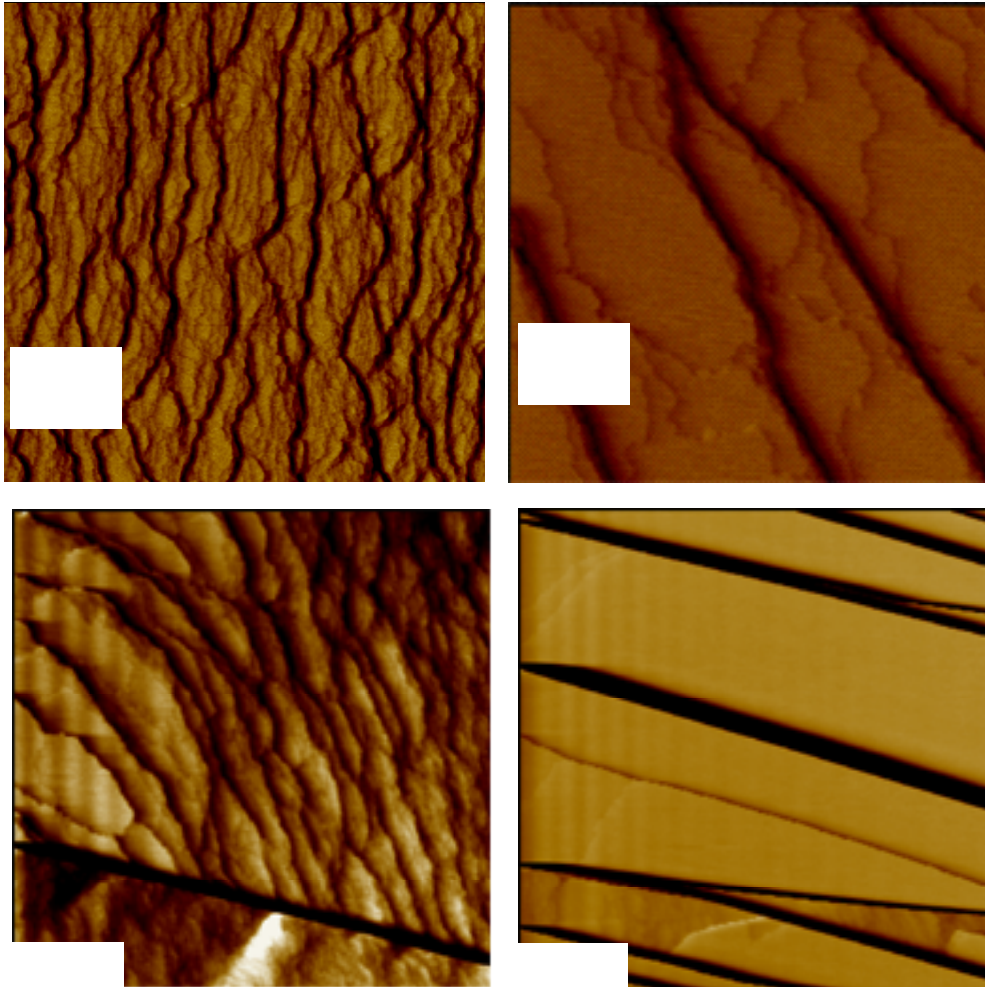
Figure 3: Changes in growth morphology with supersaturation in solutions doped with 15·10⁻⁶ mole Al per mole KDP at various points along the growth curve. (a) in the dead zone, σ = 4.1%, 7 μm scan size (b) at σ^*, σ = 6.1%, 3 μm scan size (c) during resurrection, σ = 6.2%, 10 μm scan size (d) after the velocity has rejoined that of an undoped system, σ = 8%, 15 μm scan size. In (c) a superstep is seen on the lower portion of the image. (Note: for all $\sigma>\sigma^*$, the surface grows only as a series of supersteps)

Effect of Al(III) adsorbates on growth

Solutions doped with Al(III) (shown in Figure 2 and Figure 3 a-d) affect the surface very differently than solutions doped with Fe(III). Unlike Fe(III), Al(III)-doped experiments show no slow increase in velocity in the range of $\sigma_d<\sigma<\sigma^*$, so that $\sigma_d=\sigma^*$. For all $\sigma<\sigma^*$, the surface is comprised of pinned elementary steps and macrosteps (Figure 3a). At σ^*, macrosteps only briefly recover motion while the elementary steps remain pinned (Figure 3b). Just as the macrosteps begin to move, supersteps appear and quickly cover the existing surface. The step bunches left behind by the superstep begin to move, but are again covered by the next advancing superstep. This behavior continues over a very small transition region of approximately 0.1% supersaturation (Figure 3c). Above σ^*, supersteps dominate the growth surface and, within a range of 0.2% supersaturation, the step velocity

increases to that of a undoped KDP surface at the same supersaturation (Figure 3d). For the remainder of the supersaturation range investigated, supersteps are primarily responsible for growth.

We have found that labile phosphato-complexes of Fe(III), Al(III), and Cr(III) cause step velocities to decrease and form a velocity dead zone on the {100} face of KDP at low supersaturations. The characteristic time for adsorption of the complex can be derived from the relationship between velocity and supersaturation, and is related to the morphology of the surface during the growth process. Fe(III)-doped surfaces show a unique dead zone that is not predicted by the C-V model and results from the long time scale needed for Fe(III) to reach equilibrium adsorbate concentrations on terraces ($\tau_{Fe} \sim$10-100 sec). The pinning of elementary steps causes macrosteps to form that are responsible for growth of the surface. Only in the presence of high concentrations of Fe(III) do supersteps form.

The behavior of the Al(III) adsorbate on the surface and the rapid adsorbate build-up on the terrace ($2 \cdot 10^{-4} < \tau_{Al} < 6 \cdot 10^{-4}$ s) leads to the formation of macrosteps and supersteps which are ultimately responsible for the resurrection of the surface. This observation is contrary to the C-V model, which states that the surface would be resurrected by elementary steps. The step velocities on the Al(III) doped surface resurrect solely by the propagation of supersteps that dominate growth for all $\sigma > \sigma^*$. Cr(III) doped surfaces behave much in the same way as do the Al(III) doped surfaces, including the formation and motion of supersteps during the recovery from the dead zone. Cr(III) adsorbates also have similar characteristic adsorption times ($\sim 2 \cdot 10^{-4} < \tau_{Cr} < 6 \cdot 10^{-4}$ s). The primary difference between the Al(III) and Cr(III) doped surfaces is the morphology of the growth surface after velocities resurrect from the dead zone. Cr(III) adsorbates induce the expression of supersteps only during the resurrection from the dead zone. However, after the velocity recovers, the surface is once again dominated by the motion of macrosteps. The relationship between σ^* and n is best described by a root dependence for Cr(III) and a linear dependence for Al(III)-doped solution and could be a result of the stoichiometry of the adsorbate complex.

Molecular modeling of aluminum incorporation in the KDP lattice

The need for habit control has led to interest in the step-pinning mechanisms that cause growth inhibition of the {100} face. Model systems representing five stepped KDP {100} surfaces have been prepared and studied using ab initio quantum methods. In addition, computational studies of the binding of $AlHPO_4^+$ complexes to KDP surfaces were performed using Hartree-Fock (HF) calculations. Computational chemistry methods (HF optimization using the LACVD basis set via the Jaguar program) were employed to determine binding energies and geometries of optimized aluminum phosphate complexes to KDP surfaces. Estimates of binding energies are made by computing E(cluster)- E(ligand)-E(cluster w/o ligand) where the latter are computed as single-point energies. Estimated Binding Energies for $AlHPO_4$ to steps on the (100) Face of KDP (kcal/mol) were -215 to -340kcal/mol. The relative binding energies can be integrated into the KMC calculations on impurity step interactions. Insight into the energy and geometry of complex-

surface system obtained from these calculations can be used, in conjunctions with the AFM and surface chemistry studies, to gain an understanding of the preferential binding of hydrated ionic complexes of iron and aluminum phosphates to the (100) rather than to (101) surfaces of KDP.

Steps terminated by phosphate ions are found to be less energetically favorable than their potassium-terminated counterparts. In addition, surface layer removal energies for the {100} face and the potassium-bounded and phosphate-bounded {101} faces are reported. The potassium-bounded {101} face is found to have a greater surface removal energy than the unexpressed phosphate-bounded {101} face.

We have studied five possible steps on the {100} face of KDP (see Figure 4) using ab initio quantum methods, and we have presented energetic data which may be useful in theoretical modeling of KDP crystal growth [18,19]. We have presented estimated surface removal energies for the {100} and {101} faces, as well, and we have confirmed that the K^+-bounded {101} face has a higher surface removal energy than the $H_2PO_4^-$-bounded {101} face. We have found that the steps terminated by phosphate ions, V' and D', are less energetically favorable than their potassium-terminated counterparts, V and D, according to both ion removal and column removal energies. Given the greater relative stability of step V, we do not expect that the vertical step V' will be present on the growing {100} face. The estimated column removal energies for the diagonal steps (D and D') are comparable; we do not necessarily exclude the possibility that D' steps may be present in addition to D steps. The D steps do have greater ion and column removal energies than the D' steps, as an inheritance from the two {101} faces they generate. As the focus of future work, we intend to explore candidate sites for Al^{3+} adsorption onto KDP {100} steps and to investigate the impact of the dopant species on the local step structure.
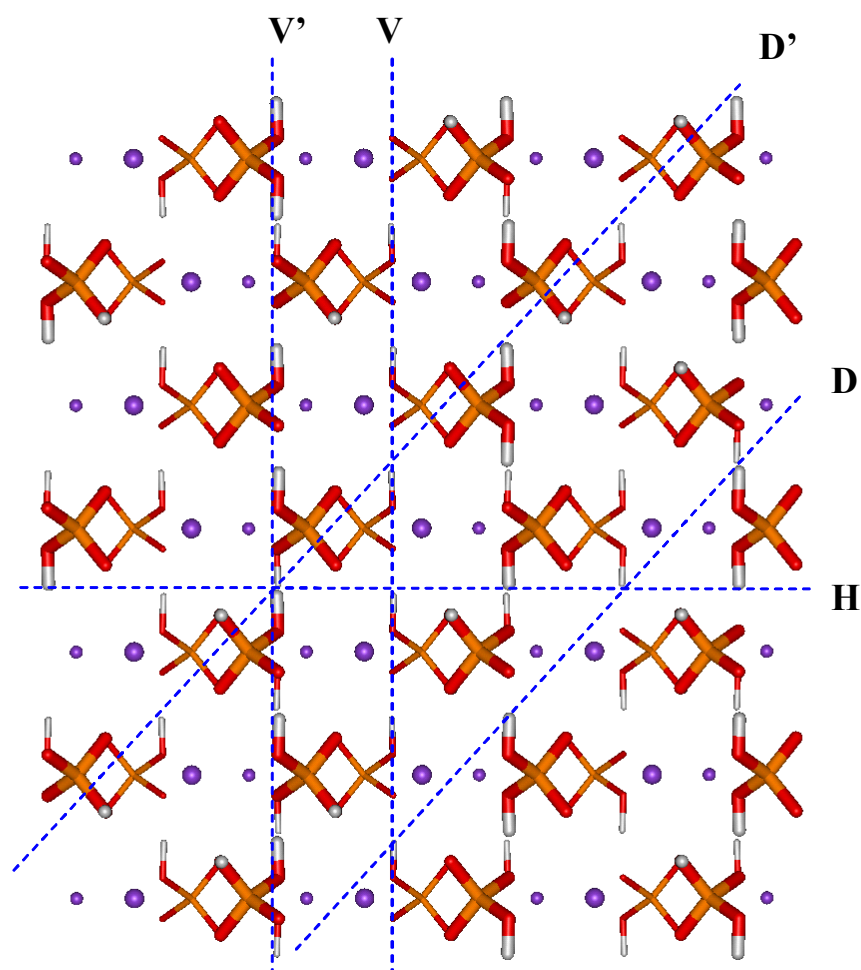
Fig. 4. Possible Steps on the Prismatic {100} Face of KDP. The top-layer ions are enlarged to aid in visualization. The steps are made by cutting away the top layer of ions along the axes indicated. The steps are denoted Horizontal (H), Vertical/K^+-terminated(V), Vertical/$H_2PO_4^-$-terminated(V'), Diagonal/K^+-terminated(D), Diagonal/$H_2PO_4^-$-terminated(V'). The diagonal step (D) generates the experimentally observed {101} face at the step edge. The horizontal step (H) generates another {100} face at the step edge.

Kinetic Monte Carlo modeling of KDP step kinetics

A preliminary Monte Carlo model for simulating step motion vs. supersaturation of KDP crystals has been developed. This model takes an initial step-train configuration and evolves it in time according to prescribed adsorption/desorption probabilities for KDP growth units that depend upon supersaturation. Equilibrium conditions were determined and the model was used to calculate sticking

coefficients. The model was then used to calculate step velocities as a function of supersaturation for temperatures in the range 20 < T < 25 ºC. The velocities for the steps on both facets (prism and pyramidal) are shown in Fig. 2. Open symbols represent AFM experimental measurements[1] and closed symbols represent the results of the MC model.

As can be seen from Fig. 5, there is a very good agreement between experimental measurements and simulation results. In addition, the values for activation energies obtained from the KMC simulations agree very well with those determined by AFM. In FYO4, the KMC model will be extended to include the effect of impurities on the step distribution and evolution of multiple-height step bunches.
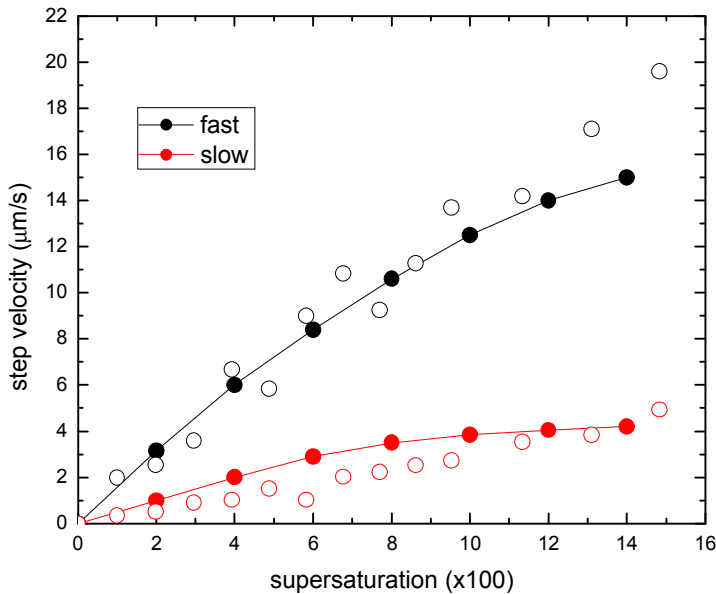

Figure 5. Step velocities vs. supersaturation. The open circles show experimental results, while the kinetic Monte Carlo predictions are show by the line and solid circles.

Summary

Through these various experiments we now have a more clear picture of how KDP crystals grow and how solution and growth conditions can be used to more favorable control the crystal habit.

Exit Plan

The immediate impact of our investigation will be to increase the quality and yield of rapid growth KDP crystals used in many photonics applications in general but specifically the large aperture Nd-glass lasers in use throughout the world. In particular this work impacts the large aperture lasers either in operation, under construction or being designed in the US, France, England, China and Japan. Within the US, the DOE laser systems at Sandia and the University of Rochester will

benefit directly from this technology because of the use of large aperture KDP and DKDP on these systems. This technology will also impact the DOE- NIF laser system that uses KDP crystals in the plasma electrode Pockels Cell (PEPC) optical switches in the main laser cavity of each of NIF's 192 laser beams. KDP is also used for the frequency doublers in the final optics assembly and deuterated KDP is used for the tripler in this assembly. The combination of these two crystals allows for the conversion of 1.06 micron wavelength laser light to the third harmonic at 351 nm, which is desirable for the high energy density and fusion ignition physics experiments planned on all of the facilities mentioned above.

In the longer term the technology we develop in this proposal can be used for rapid solution growth of a variety of crystals of importance to LLNL and national and international laser, photonics, and electro-optics programs.

References
1.   Chuck Thorsness, modeling results for KDP Large Crystal Runs*, ECMS-NIF0110148 AB/adf*

2.   Paul Ehrmann, Terry Land, Rebecca Dylla-Spears and Chuck Thorsness, Aluminum uptake by large KDP crystals, *NIF0110915 revAB/adf*

3.   R. Roza and R. Torres EDTA Method for Synthesis of Low Impurity KDP. Internal Memo Dated August 10, 1998.

4.   P. E. Miller, "Some equilibria Aspects of KDP Growth Solutions" Internal memorandum (NIF 0101124) May 20, 2003

5.   Anderson, Miller, and Thorsness. Growth kinetics of KDP at 40ºC. NIF0110941/adf

6.   Anderson, Miller, and Thorsness. Growth kinetics of KDP *NIF0111193/adf*

7.   Rashkovich, L.N.; Kronsky, N.V. *J. Cryst. Growth* 1997, *182,* 434.

8.   Land, T.A.; Martin, T.L.; Potapenko, S.; Palmore, G.T.; DeYoreo, J.J. *Nature* 1999, *399*, 442.

9.   Thomas, T.N.; Land, T.A.; Casey, W.H.; DeYoreo, J.J.   . 2004. Emergence of supersteps on KH2PO4 crystal surfaces. *PHYSICAL REVIEW LETTERS* 92 (21): art. no.-216103.

10.   Verdaguer, S.V.; Clemente, R.R. *J. Cryst. Growth* 1986, *79*, 198.

11.   Rashkovich, L.N. *KDP Family of Crystals*; Adam-Hilger: New York, 1991 and references therein

12.   Thomas, T.N., Land, T.A., Martin, T., Casey, W.H., DeYoreo, J.J., *J. Cryst. Growth,* 2003, *260*(3-4), 566.

13.   Thomas, TN; Land, TA; Johnson, M; Casey, WH. 2004. Molecular properties of adsorbates that affect the growth kinetics of archerite (KDP). *JOURNAL OF COLLOID AND INTERFACE SCIENCE* 280 (1): 18-26.

14. Stack, AG; Rustad, JR; DeYoreo, JJ; Land, TA; Casey, WH. 2004. The growth morphology of the {100} surface of KDP (archerite) on the molecular scale. *JOURNAL OF PHYSICAL CHEMISTRY B* 108 (47): 18284-18290.

15. Thomas, TN; Land, TA; DeYoreo, JJ; Casey, WH. 2004. In situ atomic force microscopy investigation of the {100} face of KH2PO4 in the presence of Fe(III), Al(III), and Cr(III). *LANGMUIR* 20 (18): 7643-7652.

16. properties of Step-Pinning Adsorbates on KDP. *GEOCHIMICA ET COSMOCHIMICA ACTA* 68 (11): A168-A168, Suppl. S.

17. Cabrera, N.; Vermilyea, D.A. *Growth and Perfection of Crystals;* Chapman and Hall: London, 1958; pg. 393.

18. Salter, E A ; Wierzbicki, A ; Land, T, Ab initio studies of stepped {100} surfaces of KDP crystals, International journal of quantum chemistry. 100, no. 5, (2004): 740 (6 pages)

19. Salter, E A ; Wierzbicki, A ; Land, T, Ab initio Study of Al(III) Adsorption on Stepped {100} Surfaces of KDP Crystals, accepted in Structural chemistry (2004)